



Title	Conditions for condensation and preservation of amorphous ice and crystallinity of astrophysical ices
Author(s)	Kouchi, A.; Yamamoto, T.; Kozasa, T.; Kuroda, T.; Greenberg, J.M.
Citation	Astronomy and Astrophysics, 290, 1009-1018
Issue Date	1994-10
Doc URL	http://hdl.handle.net/2115/42838
Rights	© 1994 ESO
Type	article
File Information	59kozasa_AA290.pdf



[Instructions for use](#)

Conditions for condensation and preservation of amorphous ice and crystallinity of astrophysical ices

A. Kouchi¹, T. Yamamoto^{2,3}, T. Kozasa², T. Kuroda^{1,*}, and J.M. Greenberg⁴

¹ Institute of Low Temperature Science, Hokkaido University, Sapporo 060, Japan

² Institute of Space and Astronautical Science, Yoshinodai 3-1-1, Sagami-hara, Kanagawa 229, Japan

³ Department of Earth and Planetary Sciences, Hokkaido University, Sapporo 060, Japan

⁴ Huygens Laboratory, University of Leiden, Niels Bohrweg 2, 2333 CA Leiden, The Netherlands

Received 6 October 1993 / Accepted 28 February 1994

Abstract. Conditions for formation and preservation of amorphous ice formed through condensation of water vapor on a substrate is investigated both theoretically and experimentally. The kinetic consideration of deposition of vapor leads to the condition for formation of amorphous ice on a cold substrate: the flux of water vapor onto the substrate should be larger than a critical flux $D_s/a^4 \equiv F_c$, where D_s is the surface diffusion coefficient of water molecules on the substrate and a the lattice constant of the substrate. The validity of the derived condition has been confirmed by measuring the critical flux of water vapor onto a substrate of polycrystalline cubic ice as a function of temperature. From the measured F_c , a surface diffusion coefficient of H₂O molecules on polycrystalline cubic ice has been determined. With regard to the preservation condition, we derive a theoretical expression of the time scale t_c for crystallization of amorphous ice, which has the same form at low temperatures as the empirical formula used so far. A self-diffusion coefficient of amorphous ice is estimated from a comparison between the theoretical and empirical formulas of t_c . The results are applied to condensation of ice in molecular clouds, circumstellar envelopes of late-type stars, and the primordial solar nebula. Discussion is given on the crystallinity of ices in these sites.

Key words: molecular processes – solar system: formation – stars: circumstellar matter – interstellar medium: clouds

1. Introduction

Ice is observed in various astrophysical sites (see Klinger 1983), and is a major component in the low-temperature environments. Understanding of ice condensation provides a basis for the study of the formation and evolution of interstellar and solar-system icy grains. So far, the equilibrium condensation theory

(e.g., Lewis 1972; Yamamoto et al. 1983) has been widely applied to estimate condensation temperatures of ice in the cosmic environments because of its simplicity. On the other hand, it has been pointed out theoretically that kinetic effects in condensation plays an essential role in determining grain characteristics such as grain size, their number density, and condensation temperatures (Yamamoto & Hasegawa 1977; Draine & Salpeter 1977; Seki & Hasegawa 1983) as well as crystalline structure (Seki & Hasegawa 1981; Gail & Sedlmayr 1984). Recently it has been pointed out that revealing whether deposited ice is amorphous or crystalline provides a key clue to the origin and thermal evolution of comets (Yamamoto 1991).

While there are many polymorphs of H₂O ice, phase relations at low temperatures and low pressures are especially relevant to discussing condensation of ice in space. The experimentally determined structure of ices formed by deposition of water vapor onto substrates at low temperatures is compiled by Hobbs (1974) as a function of temperature. According to his compilation, hexagonal ice (ice I_h) is formed as a stable phase above 170 K, metastable cubic ice (ice I_c) at temperatures between 170 and 130 K, and amorphous ice below 130 K. Most researchers presumed the transition temperature between ice I_c and amorphous ice to be 130 K (e.g., Seki & Hasegawa 1983). It should be pointed out, however, that the transition temperatures cannot be determined uniquely but have been shown experimentally to be highly dependent on the condensation rate (Olander & Rice 1972; Kouchi 1987) and pressure as well. On the other hand, the conditions for formation of amorphous Ge studied experimentally (Sloope & Tiller 1962; Krikorian & Sneed 1966) are that the growth rate should be larger than a critical value and that the substrate temperature should be lower than a critical temperature. Although there are several qualitative analyses for Ge of the effect of the growth rate on epitaxy (Krikorian & Sneed 1966) and of crystal growth in amorphous phase (Narayan 1982), these analyses are not enough to be applied to formation of amorphous solids in general, especially to amorphous ice, because they studied the growth of Ge only on the single crystal

Send offprint requests to: A. Kouchi

* Deceased

substrate. It is therefore highly desirable to clarify the formation conditions of amorphous solids that can be applicable to a wide variety of formation environments including astrophysical ones.

In the present study, we shall investigate the formation and preservation conditions of amorphous solids with particular attention to amorphous ice. On the basis of kinetics of condensation and crystal growth, we shall derive criteria for formation of amorphous solids and its preservation in Sect. 2 together with results of the experiment of condensation of amorphous ice. Comparison between the theoretical and empirical formulas for crystallization time scale is made in Sect. 3. We shall give a physical basis of the empirical formula, and evaluate a self-diffusion coefficient of amorphous ice. Crystallinity of ices in astrophysical sites is discussed in Sect. 4.

2. Formation conditions of amorphous ice

For obtaining amorphous ice the following two conditions should be satisfied: (1) formation of amorphous ice at the time of condensation, and (2) its preservation against crystallization in the relevant environment. We shall discuss the two processes separately first and combine the conditions later.

2.1. The formation condition at the time of condensation

Condensation of ice usually occurs via vapor deposition on a cold substrate. Water vapor is usually deposited on a cooled substrate in a vacuum chamber in a laboratory (Hobbs 1974) and on the grain surfaces in cosmic conditions (Seki & Hasegawa 1983). In these cases the substrate is so cold that sublimation of adsorbed vapor molecules, which are called adatoms hereafter, is negligible. Thus we assume that the sublimation time scale τ_s is much longer than the collision mean free time τ_c of adatoms diffusing on a surface of the substrate (Irisawa et al. 1990):

$$\tau_s \gg \tau_c. \quad (1)$$

Amorphous ice forms if the adatoms are “frozen” in the vicinity of each of the adsorption points and cannot settle to the crystalline configuration. Namely, amorphous ice may be formed under the condition that the diffusion distance during the time of coverage of the surface by adatoms is smaller than the lattice constant a of crystalline ice. For the impinging flux of the water vapor F , one has the coverage time t_{cover} as

$$t_{\text{cover}} = 1/Fa^2. \quad (2)$$

The diffusion distance during t_{cover} is given by $\sqrt{D_s t_{\text{cover}}}$, where D_s is the surface diffusion coefficient. Thus the formation condition of amorphous ice is expressed by

$$D_s t_{\text{cover}} < a^2, \quad (3)$$

which may be rewritten in terms of the flux F as

$$F > D_s/a^4 \equiv F_c, \quad (4)$$

which is equivalent to the condition obtained by Gail & Sedlmayr (1984).

To check the criterion (4), we made the following experiment. First a thin film of polycrystalline ice I_c , 100 to 200 Å in thickness, was prepared at 140 K by deposition of water vapor onto a metal substrate in a vacuum chamber at a pressure of 5×10^{-9} Torr by the method described previously (Kouchi 1990; Kouchi & Kuroda 1990; Kouchi et al. 1992). During an additional deposition of water vapor at a constant flux F , the substrate was cooled slowly at the rate of 0.1–1 K/min, and structural changes of the ice surface were observed in-situ by the reflection electron diffraction method using 20 keV electrons. The deposition rates were measured from separate calibration experiments by using the laser interferometry method. For varying fluxes a transition from crystalline to amorphous ice was observed to occur at varying temperatures. From these data we obtained the dependence of the critical flux F_c on the temperature T .

Figure 1 shows an example of reflection electron diffraction patterns of the surface of the ice film. In the high temperature region, the deposited ice was polycrystalline ice I_c (Fig. 1a). With decreasing substrate temperature amorphous ice began to condense at a critical temperature T (Fig. 1b). Further decrease of the substrate temperature leads to continuation of condensation of amorphous ice. These observations clearly indicate the presence of a critical flux from condensation of ice I_c to amorphous ice for a given temperature T as was predicted.

Figure 2 shows the critical flux F_c experimentally determined as a function of $1/T$, where the straight line shows a least-squares fit. The linear relation between $\ln F_c$ and $1/T$ is consistent with the theoretical prediction that F_c is proportional to the surface diffusion coefficient D_s [Eq. (4)], which is expressed by $D_s = D_{s0} \exp(-E_s/kT)$. From the measured $F_c(T)$ shown in Fig. 2, we may determine, with the use of Eq. (4), D_{s0} and E_s , and thus the surface diffusion coefficient D_s of H_2O molecules on polycrystalline ice I_c . The result is $E_s/k = 4590$ K and $D_{s0} = 1.74 \times 10^5 \text{ cm}^2 \text{ s}^{-1}$ for $a = 4.5$ Å. This surface diffusion coefficient is regarded as an upper limit, since the criterion (4) is a sufficient condition for forming amorphous ice. As will be seen in Fig. 4, D_s on polycrystalline ice I_c is much smaller than that on the (0001) face of ice I_h single crystal. This indicates that the surface of polycrystalline ice I_c is very rough on a molecular scale, which is also supported by the fact that the reflection electron diffraction pattern (Fig. 1a) is the same as the transmission one.

2.2. Formation of amorphous ice by slow vapor deposition in the laboratory

The formation condition (4) for amorphous ice that the deposition rate be larger than a critical one F_c appears at first to be completely opposite to the condition stated in Olander and Rice (1972) and confirmed by experiments performed to analyse the structure of amorphous ice (Narten et al. 1976) as well as by experiment designed to study absorption spectra (Breukers 1991). In those experiments, increasing rate of deposition

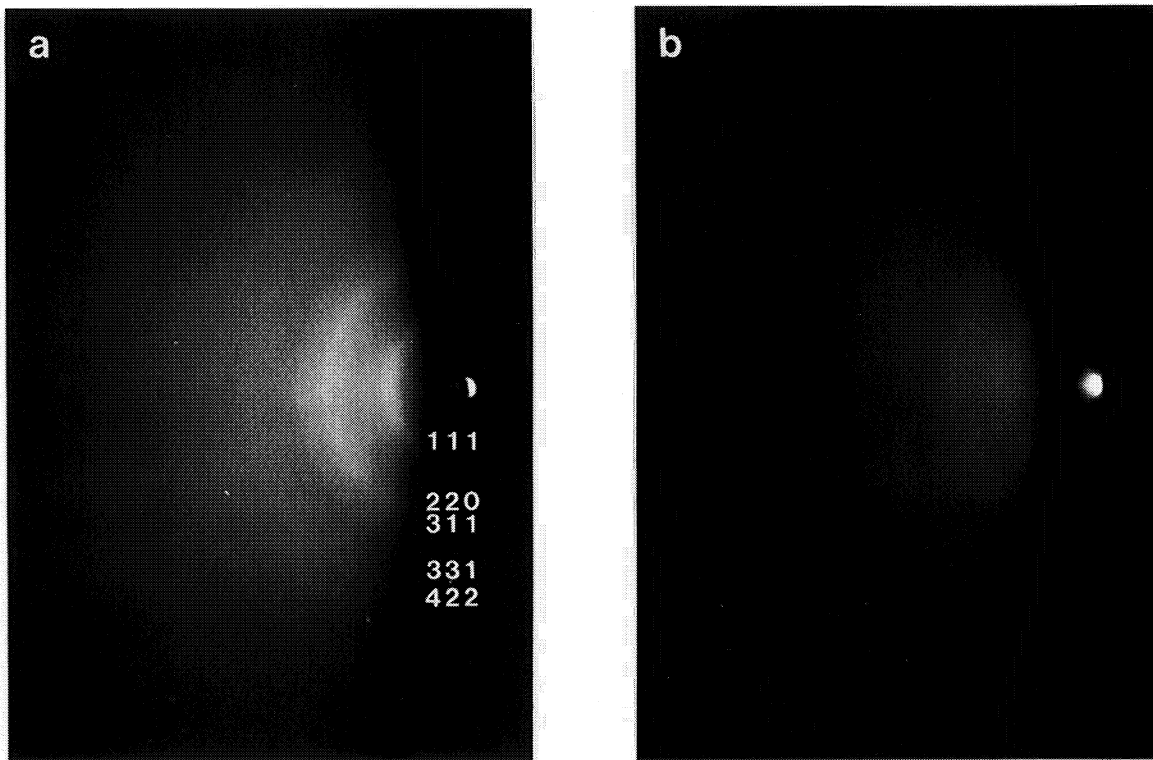


Fig. 1 a and b. Reflection electron diffraction patterns of **a** ice I_c deposited at 100 K and **b** amorphous ice deposited at 99.3 K on the surface of polycrystalline ice I_c . The deposition rate is $2 \times 10^{-8} \text{ cm s}^{-1}$

was accompanied by less and less amorphicity and ultimately to crystallinity (Kouchi et al. 1992a,b). The explanation for this apparent discrepancy with condition (4) is simply described.

The water molecule deposition is always accompanied by the release of the latent heat of fusion. With relatively thick samples the thermal conductivity of the *initially* amorphous ice is so small that localized heating cannot be transported away rapidly enough to prevent diffusion accompanying higher deposition rates and conversely. In case the sample is unshielded from the ambient room-temperature radiation field there is even less possibility for removing the heat from the local sites. As already stated the *essential* of condition (4) is that H_2O molecules may diffuse so that if local heating with increased flux *enhances* the diffusion this leads to crystallinity. A schematic of the variability of the systems leading first to decreasing and then increasing crystallinity with the flux is shown in Fig. 3 with the different regimes clearly separated. The experiments described in Sect. 2.1 lead to the condition for amorphicity with increasing flux and follow the left side of the curve in Fig. 3. The experiments described in Kouchi et al. (1992a, b) follow the right portion of the curve in Fig. 3.

2.3. Condition for preservation of amorphous ice

We shall derive the time scale for crystallization of amorphous ice on the basis of the theories of nucleation and crystalline growth. If the time scale of crystallization is longer than the

relevant time scale of the system concerned, amorphous ice will be preserved in practice.

Crystalline ice is formed through nucleation of crystalline clusters in amorphous phase and subsequent growth of the clusters. The volume fraction θ of crystalline ice at a time t depends on the nucleation rate J and the growth rate w , both of which are functions of the temperature. For constant J and w , the crystalline fraction is given from the kinetic theory of crystallization formulated by Kolmogorov (see Hobbs 1974) by

$$\theta(t) = 1 - \exp(-\alpha J w^3 t^4), \quad (5)$$

where α is a geometrical factor depending on the morphology of the crystal growth, and is given by $\alpha = 2$ for cubic growth and $\alpha = \pi/3$ for spherical growth. We define the crystallization time scale t_c by

$$t_c = (\alpha J w^3)^{-1/4}. \quad (6)$$

To compare t_c with the experimental results, we shall rewrite Eq. (6) in what follows.

The change in the Gibbs free energy ΔG for formation of a crystalline cluster of radius r in an amorphous phase is expressed by

$$\Delta G = -\frac{4\pi r^3}{3\Omega} \Delta G_v + \frac{4\pi r^2}{\Omega^{2/3}} \sigma, \quad (7)$$

where Ω is volume of a water molecule, $\sigma = \gamma \Omega^{2/3}$ with γ being the interfacial tension, and ΔG_v is the free energy difference

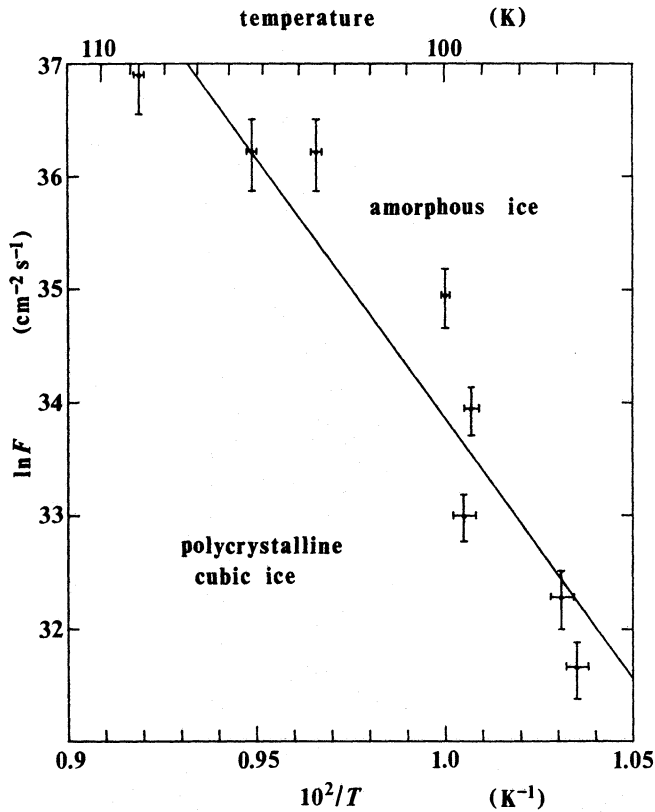


Fig. 2. Measured critical flux F_c on the surface of polycrystalline ice I_c

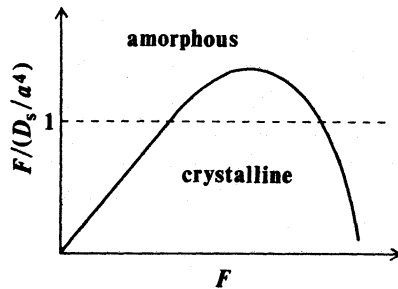


Fig. 3. Schematic drawing showing the formation condition of amorphous ice as a function of the water vapor flux F . Amorphous ice condenses in the range of F where $F/D_s a^4 > 1$ as described by the criterion (4) in the text

per molecule between bulk amorphous and crystalline ices. We approximate ΔG_v by the Clausius-Clapeyron relation between a melt (amorphous phase) and a crystal:

$$\Delta G_v = L \frac{T_m - T}{T_m}, \quad (8)$$

where L is the latent heat of crystallization per molecule at $T = 0$ K, and $T_m = 273$ K is the melting temperature. The radius r^* of a critical nucleus is given by

$$r^* = \frac{2\sigma}{\Delta G_v} \Omega^{1/3} \quad (9)$$

from $d\Delta G/dr = 0$, and the free energy difference for $r = r^*$ is given by

$$\Delta G^* = \frac{16\pi\sigma^3}{3\Delta G_v^2}. \quad (10)$$

The nucleation rate J of crystalline nuclei in amorphous phase at temperature T may be written (Seki & Hasegawa 1981) as

$$J = Z \frac{4\pi r^{*2}}{\Omega^{2/3}} \frac{D}{\Omega^{2/3}} \Omega^{-1} \exp\left(-\frac{\Delta G^*}{kT}\right), \quad (11)$$

where $Z = \Omega^{2/3}(\sigma/kT)^{1/2}/2r^{*2}$ is the Zeldovich factor, D is the self-diffusion coefficient, and k is the Boltzmann constant. With the use of Eqs. (8) and (10), J is expressed by

$$J = \frac{2\pi}{\Omega} \left(\frac{\sigma}{kT}\right)^{1/2} \frac{D_0}{\Omega^{2/3}} \exp\left[-\frac{1}{kT} \left\{ E_a + \frac{16\pi\sigma^3}{3L^2} \times \left(\frac{T_m}{T_m - T}\right)^2 \right\}\right], \quad (12)$$

where we put

$$D = D_0 \exp\left(-\frac{E_a}{kT}\right) \quad (13)$$

with E_a being the activation energy of self-diffusion.

The growth rate of crystalline clusters is given (Seki & Hasegawa 1981) by

$$w = \frac{D}{\Omega^{1/3}} \left[1 - \exp\left(-\frac{\Delta G_v}{kT}\right) \right], \quad (14)$$

where the second term in the bracket indicates the effect of remelting of the crystalline surface, and may be ignored at the low temperatures of concern here. Then w is approximated by

$$w = \frac{D_0}{\Omega^{1/3}} \exp\left(-\frac{E_a}{kT}\right). \quad (15)$$

Substituting Eqs. (12) and (15) into Eq. (6), we obtain the crystallization time scale as a function of T :

$$t_c = \left(\frac{1}{2\pi\alpha}\right)^{1/4} \left(\frac{kT}{\sigma}\right)^{1/8} \frac{\Omega^{2/3}}{D_0} \exp\left[\frac{1}{kT} \left\{ E_a + \frac{4\pi\sigma^3}{3L^2} \times \left(\frac{T_m}{T_m - T}\right)^2 \right\}\right]. \quad (16)$$

The condition for preservation of amorphous ice is that t_c is longer than the relevant time scale of the system. In other words, given the time scale t_c , a typical temperature T of the relevant system should be lower than the temperature $T_c(t_c)$:

$$T < T_c(t_c), \quad (17)$$

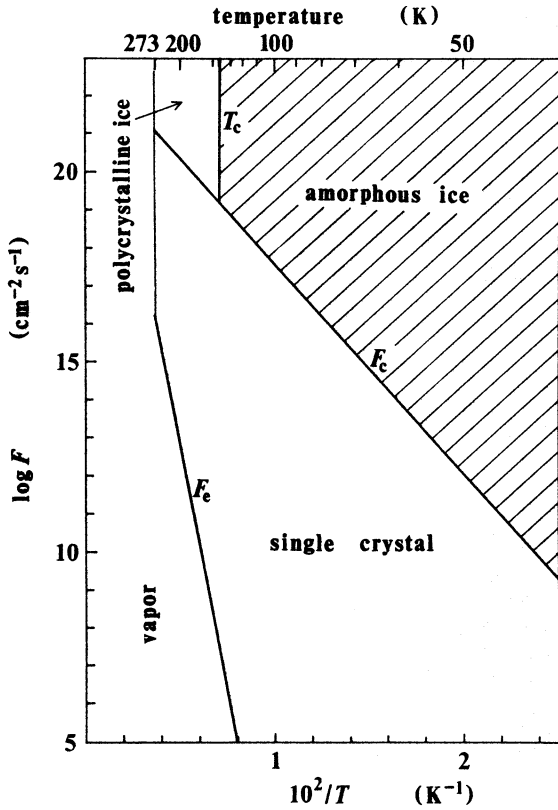


Fig. 4. Formation conditions of amorphous ice on the (0001) surface of ice I_h single crystal by vapor deposition. F_c is the critical flux, F_e the equilibrium flux, and T_c the temperature of crystallization above which the amorphous ice crystallizes in the relevant time scale t_c . Here t_c is put one hour, which is a typical time scale of the laboratory experiments

where $T_c(t_c)$ is the temperature determined from Eq. (16) for a given t_c .

It is worth pointing out that t_c given by Eq. (16) indicates that the time required for crystallization becomes shortest at a temperature T_{\min} . By ignoring the slowly varying pre-exponential factor in Eq. (16), T_{\min} is given by the solution to the following cubic equation:

$$(1 - T_{\min}/T_m)^3 + c(1 - 3T_{\min}/T_m) = 0, \\ c = 4\pi\sigma^3/3L^2E_a. \quad (18)$$

For a numerical estimate, we take for ice $L = 2.6 \times 10^{-14}$ erg/molecule ($= 9 \times 10^8$ erg g^{-1}) (Ghormley 1968), and $\gamma = 10$ erg cm^{-2} (Fletcher 1970), which give $\sigma = 1.0 \times 10^{-14}$ erg, and $E_a = 7.36 \times 10^{-13}$ erg, which will be estimated later. Then we have $c \approx 8.5 \times 10^{-3} \ll 1$ and thus $T_{\min} \approx T_m$. In this case t_c is a monotonically increasing function of T in practice. For materials with $c \gtrsim 1$, however, the crystallization time scale t_c attains a minimum well below T_m , and T_{\min} approaches $T_m/3$ for $c \gg 1$.

2.4. The combined conditions

The formation and preservation criteria given by (4) and (17) may be applied to amorphous solids in general. Here we illus-

trate the criteria for ice deposited on the substrate of ice I_h . Here ice I_h is chosen as the substrate because there have been no data of the surface diffusion coefficient D_s of H_2O molecules on any substrate except for a theoretical estimation of the activation energy on the (0001) surface of ice I_h single crystal (Kiefer & Hale 1977).

Figure 4 shows crystalline structure of ice formed on the (0001) surface of ice I_h . F_e is the equilibrium flux, i.e. the water vapor flux corresponding to the vapor pressure of ice I_h . The critical flux F_c is calculated from the relation $D_s = a^2\nu \exp(-E_s/kT)$ with the lattice constant $a = 4.5$ Å, the frequency $\nu = 2.2 \times 10^{13}$ s (Kiefer & Hale 1977), and the activation energy for the surface diffusion $E_s/k = 1230$ K (Kiefer & Hale 1977).

The crystalline structure of the ice deposited on the substrate is classified into three regimes on the F - T plane. For the flux $F_e < F < F_c$ single crystalline ice grows epitaxially on the (0001) surface of ice I_h . For $F > F_c$, on the other hand, the structure of the ice is amorphous at first. If $T > T_c$, however, crystallization of amorphous ice occurs during the relevant time interval, since t_c of Eq. (16) is smaller than the time scale of the observation. Thus the resulted structure of the ice is polycrystalline. For obtaining amorphous ice the flux and temperature conditions must be in the shaded region in Fig. 4 constrained by the criteria (4) and (17). So far, many authors have presumed that crystalline ice can be obtained only in a high temperature region (> 130 K). However, crystalline ice can also be formed at temperatures lower than 130 K when the flux is small, as is clearly seen from this figure. This conclusion is especially important for condensation of ice in a long time scale as is usually the case in astrophysical situations.

3. Discussion

The importance of knowing the self-diffusion coefficient of amorphous ice has been invoked for understanding a sublimation process of CO from amorphous H_2O -CO ice (Sandford & Allamandola 1988) and for the theoretical analysis of radiation-induced amorphization of ice crystals (Kouchi & Kuroda 1991). There has, however, been no direct measurement or estimation. We shall show that the crystallization time scale derived in Sect. 2.2 provides a method to obtain the self-diffusion coefficient D , and estimate D of amorphous ice.

Experimentally the crystallization time scale of amorphous ice has been measured as a function of the temperature ($115 \lesssim T \lesssim 145$ K) by X-ray diffraction (Dowell & Rinfret 1960), electron diffraction (Dubochet et al. 1982), and infrared spectroscopy (Hardin & Harvey 1973; Schmitt et al. 1989). The time scale of crystallization is expressed empirically by

$$t_c = A \exp(E/kT), \quad (19)$$

where A and E are constants determined from the experiments. Here we note that t_c given by Eq. (16) reduces to the same

form as the experimental formula of Eq. (19) when $T \ll T_m$. Comparison of Eq. (16) for $T \ll T_m$ with Eq. (19) yields

$$E = E_a + \frac{4\pi\sigma^3}{3L^2} \quad (20)$$

$$A = \left(\frac{1}{2\pi\alpha}\right)^{1/4} \left(\frac{kT_{\text{exp}}}{\sigma}\right)^{1/8} \frac{\Omega^{2/3}}{D_0}, \quad (21)$$

where T_{exp} is a typical temperature in the measurements. Uncertainty in the choice of T_{exp} does not much affect the value of A because of the weak dependence of A on T_{exp} .

The relations (20) and (21) imply that the self-diffusion coefficient D expressed by Eq. (13) may be determined from measured A and E . For numerical estimates we take $A = 9.54 \times 10^{-14}$ s and $E/k = 5370$ K (Schmitt et al. 1989). Other quantities that we take are $\Omega = 3.25 \times 10^{-23}$ cm³ (Yokoyama & Kuroda 1990), $L = 2.6 \times 10^{-14}$ erg/molecule (Ghormley 1968), and $\sigma = 1.0 \times 10^{-14}$ erg (Fletcher 1970). Then we have $E_a/k = 5330$ K and $D_0 = 6.1 \times 10^{-3}$ cm² s⁻¹ for the transition to cubic ice ($\alpha = 2$). It is interesting to note that the E_a -value obtained agrees with that expected from the van Liempt relation $E_a/k = 17T_m$ (e.g. Poirier 1991) for $T_m = 273$ K within a factor of 1.15.

Figure 5 compares the self-diffusion coefficient D of H₂O molecules in amorphous ice obtained here with those in ice I_h (Goto et al. 1986) and in liquid water (Wang et al. 1953) (the lines a, b, c). It is clearly seen that D of amorphous ice is larger than that of ice I_h by one to two orders of magnitude at the temperatures where amorphous ice is preserved. This suggests that, compared with ice I_h, amorphous ice has porous structure in a molecular cluster scale, which is also suggested by its very low thermal conductivity (Kouchi et al. 1992) and large surface area (Schmitt et al. 1987; Mayer & Pletzer 1986; Zhang & Buch 1990; Bar-Nun et al. 1985). However the porosity appears to be limited to only about $P = 0.1$ as derived from the infrared absorption strength of H₂O (Breukers 1991). It should be pointed out that the structure of amorphous ice not only depends on the deposition rate and deposition temperature (Olander & Rice 1972; Kouchi 1987; Zhang & Buch 1990; Narten et al. 1976) but also changes with increasing temperature. Schmitt et al. (1989) measured the crystallization time scale t_c of amorphous ices at temperatures between 125 and 140 K, which were deposited at 10 K. With increasing temperature, the structure of amorphous ice deposited at 10 K changes to another structure at around 90 and 135 K (Kouchi 1990; Laufer et al. 1987). Therefore, the self-diffusion coefficient D estimated in the present study is regarded as that of the high temperature form of amorphous ice.

Figure 5 also shows that the surface diffusion coefficients D_s of H₂O molecules on the surfaces of (0001) of ice I_h (d) and of polycrystalline ice I_c (e). One sees that D_s on polycrystalline ice is much larger than D in amorphous ice. Since the surface of amorphous ice is rougher than that of polycrystalline ice microscopically (Schmitt et al. 1987; Mayer & Pletzer 1986; Zhang & Buch 1990; Bar-Nun et al. 1985; Laufer et al. 1987), it is expected that the surface diffusion coefficient D_s on amorphous ice should be between D_s on polycrystalline ice I_c and D in amorphous ice.

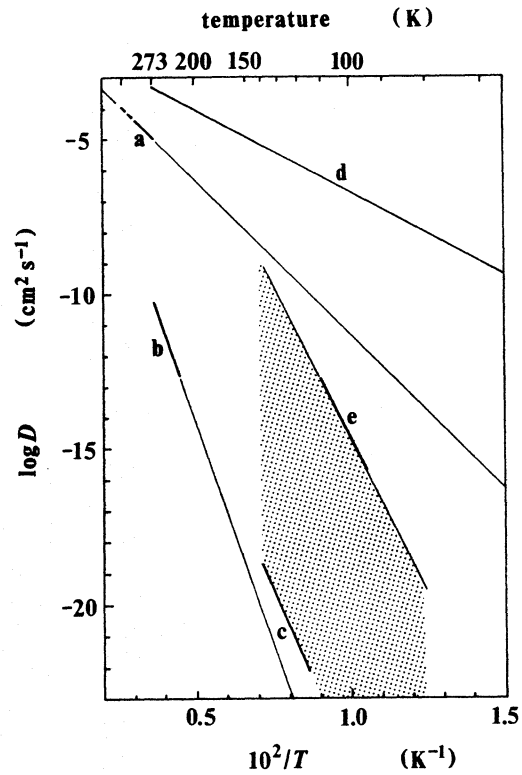


Fig. 5. Self-diffusion coefficients D of H₂O in (a) liquid water, (b) ice I_h and (c) amorphous ice, and surface diffusion coefficients of H₂O on the surfaces of (d) the (0001) face of I_h and (e) polycrystalline ice I_c. D_s on amorphous ice is expected to be in shaded part

4. Crystallinity of astrophysical ices

Crystallinity of astrophysical ice provides a clue to investigating the evolution of grains in interstellar space and the origin and evolution of the solar-system icy bodies such as cometary nuclei. In this section we briefly discuss crystallinity of astrophysical ices on the basis of the criteria described in Sect. 2.

4.1. Circumstellar envelopes

Crystalline H₂O ice is identified from the distinct emission features at 44 and 60 μ m in the circumstellar envelope of the evolved bipolar nebula IRAS 09371+1212 (Omont et al. 1990). The observation suggests the possibility of condensation of crystalline ice in circumstellar envelopes of evolved stars, although the evolutionary stage of the star is still uncertain (Robinson et al. 1992).

In circumstellar envelopes of evolved stars, water ice condenses to form icy mantles on the surfaces of refractory grains already condensed as the gas cools down with expansion. For an estimate of the impinging flux of H₂O molecules, we assume a simple model that the circumstellar envelope is spherically symmetric with constant outflow velocity v and that the temperature of the gas at the distance r from the central star is expressed by $T(r) = T_*(r_*/r)^\beta$, where the asterisk represents the values at the photosphere of the central star and β is a parameter depend-

ing on the cooling rate of the gas. Then the mass density ρ at distance r from the central star with mass loss rate \dot{M} is given by

$$\rho = \frac{\dot{M}}{4\pi r^2 v} = \left(\frac{\dot{M}}{L}\right) \frac{\sigma_S T_*^4}{v} \left(\frac{T}{T_*}\right)^{2/\beta}, \quad (22)$$

where T_* is the effective temperature of the central star, $L = 4\pi r_*^2 \sigma_S T_*^4$ its luminosity, and σ_S the Stefan-Boltzmann constant. In an envelope of an oxygen-rich star all carbon atoms are locked into CO molecules and the remaining O atoms form H₂O molecules (Jura & Morris 1985 and references therein). The concentration of H₂O molecules $n_{\text{H}_2\text{O}}$ is expressed by $n_{\text{H}_2\text{O}} = f_{\text{H}_2\text{O}} \rho / \mu m_{\text{H}}$, where μ is the mean molecular weight of the gas, $f_{\text{H}_2\text{O}}$ the number fraction of H₂O molecules, and m_{H} mass of a hydrogen atom. The impinging flux of H₂O molecules per unit surface area of the grains is given as a function of the gas temperature T by

$$\begin{aligned} F_{\text{H}_2\text{O}} &= \frac{f_{\text{H}_2\text{O}} \rho}{\mu m_{\text{H}}} \left(\frac{kT}{2\pi \mu_{\text{H}_2\text{O}} m_{\text{H}}}\right)^{1/2} \\ &= 2.4 \times 10^4 \left(\frac{2}{\mu}\right) \left(\frac{\dot{M}}{10^{-5} M_{\odot} \text{yr}^{-1}}\right) \left(\frac{10^4 L_{\odot}}{L}\right) \left(\frac{f_{\text{H}_2\text{O}}}{10^{-4}}\right) \\ &\quad \times \left(\frac{10 \text{km s}^{-1}}{v}\right) \left(\frac{T_*}{3000 \text{K}}\right)^{4-2/\beta} \\ &\quad \times \left(\frac{T}{100 \text{K}}\right)^{2/\beta+1/2} \text{cm}^{-2} \text{s}^{-1}, \quad (23) \end{aligned}$$

where $\mu_{\text{H}_2\text{O}} = 18$ is the molecular weight of an H₂O molecule. We put $\beta = 0.5$ in Eq. (23) for the numerical estimate. Calculations show that condensation of H₂O ice on silicate grains occurs at temperatures around 100 K for the parameters L ranging from 5×10^3 to $10^4 L_{\odot}$ and \dot{M} ranging from 10^{-6} to $10^{-4} M_{\odot} \text{yr}^{-1}$. The difference between the equilibrium temperature and the condensation temperature is at most 30 K in the range of the calculations.

Thus the impinging flux of H₂O molecules on substrate grains in circumstellar envelopes is $F \sim 10^4 \text{cm}^{-2} \text{s}^{-1}$ at $T = 100 \text{K}$, and is much lower than the critical flux for formation of amorphous ice $F_c = 10^{22} \text{cm}^{-2} \text{s}^{-1}$ as shown in Fig. 6. In consequence icy mantles formed in circumstellar envelopes of evolved stars is crystalline. Here we should keep in mind that the optical thickness of the circumstellar envelopes must be larger than a certain value in order for crystalline ice to be formed and preserved; otherwise interstellar UV photons penetrating into the envelope could dissociate H₂O molecules (Jura & Morris 1985), and amorphize the crystalline H₂O ice already formed (Kouchi & Kuroda 1990). In any case the kinetic consideration for the formation of amorphous ice leads to the conclusion that H₂O ice should be crystalline at the time of condensation in circumstellar envelopes of evolved stars. Note that our discussion is different from the previous discussions by Omont et al. (1990) and Robinson et al. (1992): They consider that crystalline ice is formed by crystallization of the amorphous ice mantle after the condensation, whereas our conclusion is that crystalline ice

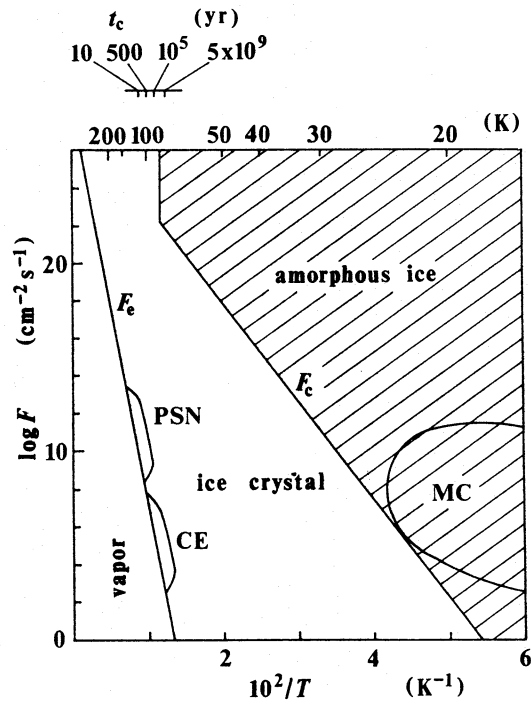


Fig. 6. Crystallinity of ices in astrophysical sites. F_c^* is the critical flux, and t_c is put 10^7 years. In upper abscissa, time scale for crystallization is shown. PSN, CE and MC denote the primordial solar nebula, circumstellar envelope and molecular cloud, respectively

is formed at the condensation because of $F < F_c$. Our conclusion is consistent with the experimental results obtained by studying the $45 \mu\text{m}$ absorption feature of ice and using it in the modelling of silicate-core ice mantle grains in the envelope of IRAS 09371+22 (Breuker 1991).

4.2. Molecular clouds

Water ice observed in molecular clouds is in an amorphous phase, which is concluded from the broad absorption feature around $3.1 \mu\text{m}$ in comparison with the spectral feature of crystalline H₂O ice (e.g. van de Bult et al. 1985; Hagen et al. 1981; Whittet 1992).

In molecular clouds the temperature of grains is so low (typically $\sim 10 \text{K}$) that most molecules as well as atoms which strike their surface will stick. The formation of H₂O molecules as a mantle on the grain occurs primarily as a result of sequential surface reactions of $\text{O} + \text{H} \rightarrow \text{OH}$ and $\text{OH} + \text{H} \rightarrow \text{H}_2\text{O}$. The rate at which this occurs can be described as a flux of H₂O molecules derived from sticking of O atoms:

$$\begin{aligned} F_{\text{H}_2\text{O}} &= n_{\text{H}_2} f_{\text{O}} \left(\frac{kT}{2\pi \mu_{\text{O}} m_{\text{H}}}\right)^{1/2} \\ &= 2.7 \times 10^3 \left(\frac{n_{\text{H}_2}}{10^4 \text{cm}^{-3}}\right) \left(\frac{f_{\text{O}}}{10^{-4}}\right) \\ &\quad \times \left(\frac{T}{10 \text{K}}\right)^{1/2} \text{cm}^{-2} \text{s}^{-1}. \quad (24) \end{aligned}$$

However, at each stage of surface reactions an energy release on the order of an eV occurs which locally heats the surface. This will lead to a possible displacement of the H₂O molecule formed. An upper limit of the displacement is estimated in the Appendix, in which the surface diffusion distance induced by heating due to molecule formation is calculated. The result shows that the displacement is less than $2a$ because the temperature decreases rapidly with increasing distance from the formation point and consequently so does the surface diffusion coefficient. Thus the *effective* impinging flux of water molecules fulfills the requirement for amorphous ice formation as shown in Fig. 6. Furthermore the crystallization time scale estimated from Eq. (16) is much longer than the cloud lifetime of $\sim 10^7$ yr for the grain temperature of ~ 10 K in molecular clouds. Therefore the criteria (4) and (17) lead to the presence of amorphous ice in molecular clouds, as is consistent with the observations.

4.3. The primordial solar nebula

To discuss crystallinity of ice in the primordial solar nebula, one has to know the temperature history during formation of the solar nebula. But the details are still uncertain. In view of the present theory of formation of the primordial solar nebula (e.g. Hayashi et al. 1985), we simplify the temperature history to the two stages as schematically shown in Fig. 7: (1) Heating followed by cooling at the stage of the solar nebula formation. The heating is caused by shock waves induced by infalling of the gas in the parent molecular cloud onto the nebular disk surfaces. The cooling is due to thermal emission from the nebular surfaces. (2) A steady stage, which is reached after the cooling of the solar nebula. We shall estimate (a) the maximum temperature for preservation of amorphous ice in the parent molecular cloud at stage (1), (b) the region in the solar nebula where amorphous ice is preserved, and (c) crystallinity of the ice recondensed in the cooling of the solar nebula.

First we estimate (a) the temperature for preservation of amorphous ice in the parent molecular cloud. The ice in the parent molecular cloud could crystallize by heating at stage (1). The crystalline fraction θ given by Eq. (5) is that for a constant temperature. When the temperature varies with time, the change in the nucleation rate J and the growth rate w should be taken into account, which leads to a rather complicated formula. Instead we adopt a phenomenological approach and write down the equation describing the rate of the change in the crystallization degree (Haruyama et al. 1993) as

$$\frac{\partial \theta}{\partial t} = \frac{1 - \theta}{t_c} = \frac{(1 - \theta)e^{-E/kT}}{A}, \quad (25)$$

where t_c is the crystallization time scale given by Eq. (19). Integration of Eq. (25) leads to

$$1 - \theta = \exp\left(-\frac{1}{A} \int_0^t e^{-E/kT} dt\right). \quad (26)$$

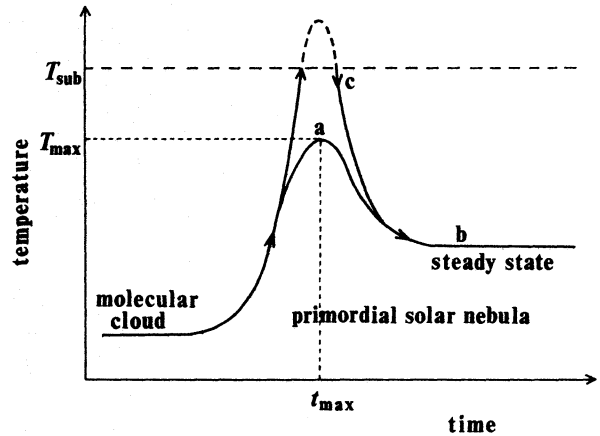


Fig. 7. Schematic thermal history from molecular cloud to the primordial solar nebula

Since the crystallization rate $1/t_c = A^{-1}e^{-E/kT}$ is a rapidly increasing function of T , the crystallization proceeds most efficiently near the maximum temperature T_{\max} in the course of heating of the solar nebula. In other words the integrand has a sharp peak at $t = t_{\max}$, the time of the maximum temperature T_{\max} . The integration may thus be carried out with the use of the conventional saddle-point method, and one obtains

$$1 - \theta = \exp\left[-\left\{\frac{2\pi k}{E(-\partial^2 T/\partial t^2)_{t_{\max}}}\right\}^{1/2} \times \frac{T_{\max}}{A} e^{-E/kT_{\max}}\right]. \quad (27)$$

Substantial crystallization occurs when the maximum temperature reached is higher than T_{\max} determined by

$$\left\{\frac{2\pi k}{E(-\partial^2 T/\partial t^2)_{t_{\max}}}\right\}^{1/2} \frac{T_{\max}}{A} e^{-E/kT_{\max}} = 1. \quad (28)$$

We evaluate $(-\partial^2 T/\partial t^2)_{t_{\max}}$ in Eq. (28) roughly to be $\sim \Delta T/t_{\text{heat}}^2$, where $\Delta T \sim 100$ K is the temperature elevation and t_{heat} is the heating time scale. According to a model of the solar nebula formation (e.g. Hayashi et al. 1985), the parent molecular cloud collapses isothermally up to the gas density of $\sim 10^{-13}$ g cm⁻³. Afterward the temperature of the gas increases with increasing density of the cloud. A shortest estimate of t_{heat} may be taken as the free-fall time from the gas density $\sim 10^{-13}$ g cm⁻³, which gives $t_{\text{heat}} \sim 10^{10}$ s. An upper limit of the time scale, on the other hand, may be taken as the lifetime of the molecular cloud, i.e. $t_{\text{heat}} \sim 10^{15}$ s. Thus $(-\partial^2 T/\partial t^2)_{t_{\max}}$ would be in the interval of 10^{-8} to 10^{-13} K s⁻².

The temperature T_{\max} is calculated for a wide range of $(-\partial^2 T/\partial t^2)_{t_{\max}}$ of 10^{-8} to 10^{-13} K s⁻². It is found that T_{\max} is insensitive to $(-\partial^2 T/\partial t^2)_{t_{\max}}$ and is 110 to 120 K. Note that these temperatures are rather close to the sublimation temperature of ice, implying that amorphous ice in the molecular cloud is preserved so long as it survived without sublimation.

The amorphous ice which survived during the formation of the solar nebula enters the stage of the steady-state solar nebula (see Fig. 7), in which crystallization proceeds at a rate depending

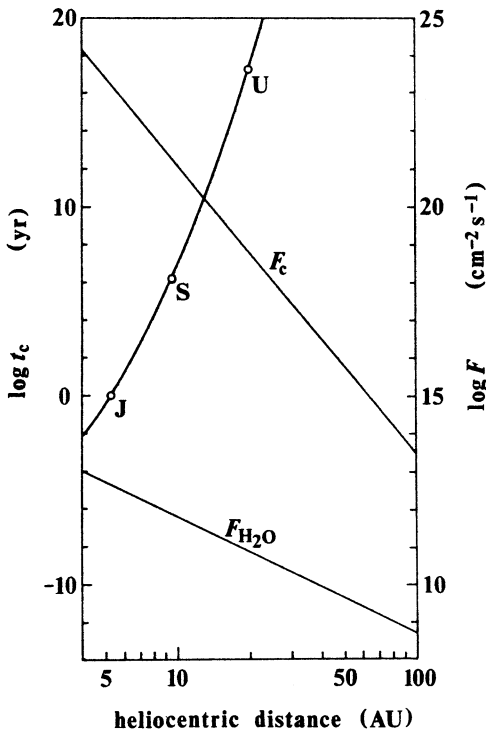


Fig. 8. Crystallization time scale t_c of amorphous ice in the primordial solar nebula (the left ordinate). The arrows labeled by J, S, U, ... indicate the present heliocentric distance of Jupiter, Saturn, Uranus, ... Flux of H_2O molecules $F_{\text{H}_2\text{O}}$ for the case of recondensation also shown together with the critical flux F_c (the right ordinate)

on the temperature where the ice is placed. We discuss (b) the region in the solar nebula where amorphous ice is preserved during the lifetime of the solar nebula. To get a quantitative picture, one requires the solar nebula model which gives the temperature distribution. We adopt the steady nebula model by Hayashi (1981), in which the temperature at heliocentric distance r is given by

$$T(r) = 280(\text{AU}/r)^{1/2} \text{ K}. \quad (29)$$

The crystallization time scale calculated from Eq. (19) together with Eq. (29) is shown as a function of the heliocentric distance r in Fig. 8. It is seen that amorphous ice is preserved in the region where $r > 12$ AU; i.e., outside the Saturnian region, during the nebular lifetime of $\sim 10^8$ yr. This implies that icy grains which formed the Uranian and Neptunian satellites and comets were initially amorphous, if they were formed from the icy grains preserved from the molecular cloud stage.

Finally we discuss (c) the crystallinity of ice recondensed in the solar nebula. The present theories of the solar nebula formation have not clarified which region in the solar nebula was heated up to the temperature above the sublimation temperature of ice. One may expect that the temperature in the inner region of the nebula rose enough at stage (1) that ice in the parent cloud sublimed and did not recondense even at stage (2). The region where ice could exist is limited to the region beyond the asteroidal belt (Hayashi 1981). There is an alternative possibility

that ice in the parent molecular cloud first sublimed during the formation of the solar nebula and subsequently recondensed when the solar nebula cooled down (see Fig. 7), in contrast with the case of the preservation of ice in the parent cloud discussed above. The ice condenses on the surface of the pre-existing refractory grains as in the case of circumstellar envelopes. The impinging flux of H_2O molecules is given by

$$\begin{aligned} F_{\text{H}_2\text{O}} &= n_{\text{H}_2}(r) f_{\text{H}_2\text{O}} \left(\frac{kT}{2\pi\mu_{\text{H}_2\text{O}}m_{\text{H}}} \right)^{1/2} \\ &= 6.4 \times 10^{14} \left(\frac{r}{\text{AU}} \right)^{-3} \left(\frac{f_{\text{H}_2\text{O}}}{10^{-4}} \right) \text{ cm}^{-2}\text{s}^{-1}, \end{aligned} \quad (30)$$

where the gas density $n_{\text{H}_2}(r)$ as a function of the heliocentric distance r is taken from the Hayashi model (1981), which gives $n_{\text{H}_2}(r) = 4.4 \times 10^{14} (r/\text{AU})^{-11/4} \text{ cm}^{-3}$ at the midplane of the solar nebula. This flux is compared with the critical flux F_c given by the criterion (4). The result is shown in Fig. 8, which indicates that crystalline ice forms in the whole region of the solar nebula in contrast with the case of the preservation of amorphous ice in the parent molecular cloud.

Acknowledgements. We wish to dedicate this paper to the late Professor Toshio Kuroda. We thank T. Kadono and M. Abe for helpful discussion. We thank the Netherlands Organization for Scientific Research and the Japan Society for the Promotion of Science for support under an exchange program. Part of this research was supported by a Grant-in-Aid for Scientific Research from the Japanese Ministry of Education, Science and Culture and by a NASA grant #NGR 33018148. One of us (A.K.) was also supported by the Yamada Science Foundation, Japan.

Appendix: upper limit of the diffusion distance of an H_2O molecule formed on the grain surface

Consider an H_2O molecule formed at $t = 0$, $r = 0$ on the surface, where energy E is released instantaneously. We assume that the energy E is transferred to the grain by conduction, and approximate the grain surface by a plane. The temperature at distance r from the formation point at time t is then given by a solution of the equation of heat conduction as

$$T(r, t) = \frac{E}{4\rho c_p (\pi\chi t)^{3/2}} \exp\left(-\frac{r^2}{4\chi t}\right), \quad (A1)$$

where ρ is the density of the grain material, c_p is the specific heat per unit mass, and χ is the thermal diffusivity, and ρc_p and χ are assumed to be constant. From Eq. (A1) one sees that at a given distance r the temperature reaches a maximum of

$$T_{\text{max}} = \left(\frac{6}{\pi e}\right)^{3/2} \frac{E}{4\rho c_p r^3} \quad (A2)$$

at a time $t_{\text{max}} = r^2/6\chi$. Furthermore it should be kept in mind that the temperature $T(r_1, t)$ is always higher than the temperature $T(r_2, t)$ for $r_1 < r_2$.

For accurate evaluation of the surface diffusion distance of a molecule formed at $r = 0$ with the energy release E , one has to solve the diffusion equation where the diffusion coefficient,

which is a function of temperature given by Eq. (A1), varies with time t and distance r . Here we estimate an upper limit of the diffusion distance in a simple manner, which is sufficient for the present purpose.

First we investigate the surface diffusion distance of an H_2O molecule initially placed at distance r . An upper limit of the diffusion distance d_{max} may be written as

$$d_{\text{max}}^2(r) = \int_0^\infty D_s dt = a^2 \nu \int_0^\infty e^{-E_s/kT(r,t)} dt. \quad (\text{A3})$$

The actual diffusion distance of a molecule placed at r at $t = 0$ is smaller than $d_{\text{max}}(r)$ given by Eq. (A3), since the temperature becomes lower as the molecule diffuses to a point at $> r$ and thus the diffusion coefficient decreases compared with that at the initial point r . Since the temperature $T(r, t)$ given by Eq. (A1) has a sharp maximum T_{max} at time t_{max} , the integration may be carried out by the saddle point method. The result is given by

$$\frac{d_{\text{max}}^2}{a^2} = \frac{a^2 \nu}{\chi} \left(\frac{\pi}{27K} \right)^{1/2} x^{1/2} e^{-Kx^3} \quad \text{with } x \equiv r/a \text{ and} \quad (\text{A4})$$

$$\begin{aligned} K &\equiv \frac{E_s}{kT_{\text{max}}(r=a)} = 4 \left(\frac{\pi e}{6} \right)^{3/2} \frac{\rho c_p E_s a^3}{kE} \\ &= 3.87 \left(\frac{\rho}{\text{g cm}^{-3}} \right) \left(\frac{c_p}{10^7 \text{ erg g}^{-1} \text{ K}^{-1}} \right) \left(\frac{E_s/k}{10^3 \text{ K}} \right) \\ &\quad \times \left(\frac{a}{4.5 \text{ \AA}} \right)^3 \left(\frac{eV}{E} \right). \end{aligned} \quad (\text{A5})$$

For representative values of $K = 3.87$, $a = 4.5 \text{ \AA}$, and $\nu = 10^{13} \text{ s}^{-1}$, and a lower limit of $\chi = 8.9 \times 10^{-8} \text{ cm}^2 \text{ s}^{-1}$, which is the thermal diffusivity of amorphous ice (Kouchi et al. 1992; see also Haruyama et al. 1993), we have $d_{\text{max}}^2/a^2 \simeq 2 \times 10^{-9} \ll 1$ for $x = 2$ and much smaller values for $x > 2$, indicating that molecules initially placed at $x \geq 2$ remain there even after the heat of formation has passed through. We denote by r_m the minimum distance where d_{max}^2/a^2 becomes less than unity. For the above estimate $r_m = 2a$.

Next let us imagine the situation that a molecule formed at $r = 0$ and $t = 0$ diffuses to the distance $r = r_m$ at a time t_m . The diffusion distance of the molecule after the time t_m is less than a by the definition of r_m . Thus a molecule formed at $r = 0$ cannot diffuse to the distance larger than r_m . The r_m is less than $2a$ for the parameter values adopted above, and even if we take K as small as $K = 1$, $r_m = 3a$. In conclusion the molecules formed are confined in the immediate vicinity of the formation place in general.

References

- Bar-Nun A., Herman G., Laufer D., 1985, *Icarus* 63, 317
 Breukers R., 1991, Ph. D. Thesis, University of Leiden
 Dowell L.G., Rinfret A.P., 1960, *Nat* 188, 1144
 Dubochet J., Lepault L., Freeman R., Berriman J.A., Homo J.C., 1982, *J. Microsc.* 128, 219
 Fletcher N.H., 1970, *The Chemical Physics of Ice*. Cambridge Univ. Press, London
 Gail H.-P., Sedlmayr E., 1984, *A&A* 132, 163
 Ghormley J.A., 1968, *J. Chem. Phys.* 48, 503
 Goto K., Hondoh T., Higashi A., 1986, *Jpn. J. Appl. Phys.* 25, 351
 Hardin A.H., Harvey K.B., 1973 *Spectrochim. Acta* 29A, 1139
 Haruyama J., Yamamoto T., Mizutani H., Greenberg J.M., 1993, *J. Geophys. Res. (Planets)*, 98E, 15079
 Hayashi, C., 1981, *Prog. Theor. Phys. Suppl.* 70, 35
 Hayashi C., Nakazawa K., Nakagawa Y., 1985, in: *Protostars & Planets II*, Black D.C., Matthews M.S. (eds.), Univ. Arizona Press, Tucson, p. 1100
 Hagen W., Tielens A.G.G.M., Greenberg J.M., 1981, *Chem. Phys.* 56, 367
 Hobbs P.V., 1974, *Ice Physics*, Oxford Univ. Press, London
 Irisawa T., Arima Y., Kuroda T., 1990, *J. Cryst. Growth*, 99, 491
 Jura M., Morris M., 1985, *ApJ*, 292, 487
 Kiefer J., Hale B.N., 1977, *J. Chem. Phys.*, 67, 3206
 Klinger J., 1983 *J. Phys. Chem.* 87, 4209
 Kouchi A., 1987, *Nat* 330, 550
 Kouchi A., 1990, *J. Cryst. Growth* 99, 1220
 Kouchi A., Greenberg J.M., Yamamoto T., Mukai T., 1992a, *ApJ* 388, L73
 Kouchi A., Greenberg, J.M., Yamamoto, T., Mukai, T., Xing, Z.F., 1992b, *In Physics and Chemistry of Ice*, Maeno N., Hondoh, T. (eds.) Hokkaido Univ. Press, Sapporo, p. 229
 Kouchi A., Kuroda, T., 1990, *Nat* 344, 134
 Kouchi A., Kuroda T., 1991, in: *Origin and Evolution of Interplanetary Dust*, Levasseur-Regourd A.C., Hasegawa H. (eds.), Kluwer Academic Press, Dordrecht, p.87
 Krikorian E., Sneed R. J., 1966, *J. Appl. Phys.* 37, 3665
 Laufer D., Kochavi E., Bar-Nun A., 1987, *Phys. Rev.* B35, 2427
 Lewis J.S., 1972, *Icarus* 16, 241
 Mayer E., Pletzer R., 1986, *Nat* 319, 298
 Narayan J., 1982, *J. Appl. Phys.* 53, 8607
 Narten A.H., Venkatesh C.G., Rice, S.A., 1976, *J. Chem. Phys.* 64, 1106
 Olander D.S., Rice S.A., 1972, *Proc. Nat. Acad. Sci.* 69, 98
 Omont A., Moseley S.H., Forveille T., et al., 1990, *ApJ*. 355, L27
 Poirier J.-P., 1991, *Introduction to the Physics in the Earth's Interior*, Cambridge Univ. Press, p. 143
 Robinson G., Smith R. G., Hyland A., 1992, *MNRAS* 256, 437
 Sandford S.A., Allamandola L.J., 1988, *Icarus* 76, 201
 Schmitt B., Espinasse S., Grim R.A.J., Greenberg J.M., Klinger J., 1989, *ESA SP-302*, 65
 Schmitt B., Ocampo J., Klinger J., 1987, *J. Phys. (Paris)* 48 C1, 519
 Seki J., Hasegawa H., 1981, *Prog. Theor. Phys.* 66, 903
 Seki J., Hasegawa H., 1983, *Ap&SS* 94, 177
 Sloop B.W., Tiller C.O., 1962, *J. Appl. Phys.* 33, 3458
 van de Bult C.E.P.M., Greenberg J.M., Whittet, D.C.B., 1985, *MNRAS* 214, 289
 Wang J.H., Robinson C.V., Edelman I.S.J., 1953, *Am. Chem. Soc.* 75, 466
 Whittet D.C.B., 1992, *Dust in the Galactic Environment*, Institute of Physics Publishing, Bristol
 Yamamoto T., 1991, in: *Comets in the Post-Halley Era*, Newburn R., Neugebauer M., Rahe J. (eds.), Kluwer Academic Press, Dordrecht, p. 361
 Yamamoto T., Hasegawa H., 1977, *Prog. Theor. Phys.* 58, 816
 Yamamoto T., Nakagawa N., Fukui Y., 1983, *A&A* 122, 171
 Yokoyama E., Kuroda T., 1990, *Phys. Rev.* A41, 2038
 Zhang, Q., Buch, V., 1990, *J. Chem. Phys.* 92, 5004